Atmospheric Environment 131 (2016) 269–278

Contents lists available at ScienceDirect

Atmospheric Environment

journal homepage: www.elsevier.com/locate/atmosenv

Laboratory testing of airborne brake wear particle emissions using a dynamometer system under urban city driving cycles

Hiroyuki Hagino*, Motoaki Oyama, Sousuke Sasaki

Energy and Environment Research Division, Japan Automobile Research Institute, 2530 Karima, Tsukuba, Ibaraki 305-0822, Japan

HIGHLIGHTS

- A laboratory brake dynamometer system measured brake wear particle emissions.
- Particle emissions were measured during urban city driving cycles.
- Key tracers of brake wear particle emissions include Fe, Cu, Ba, and Sb.

GRAPHICAL ABSTRACT

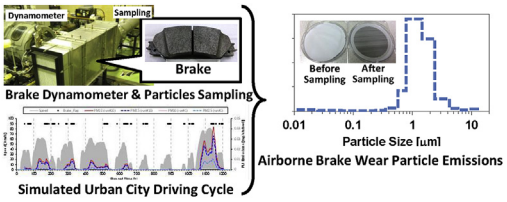

ARTICLE INFO

Article history:
Received 17 October 2015
Received in revised form
6 February 2016
Accepted 10 February 2016
Available online 12 February 2016

Keywords:
Brake wear debris
Brake abrasion dust
Oxygenated organic aerosol
Atmospheric antimony (Sb) emissions

ABSTRACT

To measure driving-distance-based mass emission factors for airborne brake wear particulate matter (PM; i.e., brake wear particles) related to the non-asbestos organic friction of brake assembly materials (pads and lining), and to characterize the components of brake wear particles, a brake wear dynamometer with a constant-volume sampling system was developed. Only a limited number of studies have investigated brake emissions under urban city driving cycles that correspond to the tailpipe emission test (i.e., JC08 or JE05 mode of Japanese tailpipe emission test cycles). The tests were performed using two passenger cars and one middle-class truck. The observed airborne brake wear particle emissions ranged from 0.04 to 1.4 mg/km/vehicle for PM_{10} (particles up to 10 μm (in size), and from 0.04 to 1.2 mg/km/vehicle for $PM_{2.5}$. The proportion of brake wear debris emitted as airborne brake wear particles was 2–21% of the mass of wear. Oxygenated carbonaceous components were included in the airborne PM but not in the original friction material, which indicates that changes in carbon composition occurred during the abrasion process. Furthermore, this study identified the key tracers of brake wear particles (e.g., Fe, Cu, Ba, and Sb) at emission levels comparable to traffic-related atmospheric environments.

1. Introduction

Particulate matter (PM) in the atmosphere is an important component of air pollution that can cause adverse health effects (Dockery and Pope, 2006). PM comprises a complex mixture of components derived from different sources, with motor vehicle emissions being one of the most important sources in urban areas (Pierson and Brachaczek, 1983). PM originating from motor vehicles is categorized based on two main sources: exhaust emissions (e.g., vehicle tailpipe emissions) that represent PM resulting from incomplete fuel combustion and lubricant volatilization during the combustion processes; and non-exhaust emissions created through brake, tire, and general vehicle wear processes and through the resuspension of road wear particles (Thorpe and Harrison, 2008). Several studies using road tunnels and/or roadside environments have shown that automotive brake abrasion dust (hereafter called brake wear particles) is an important source of PM originating from

* Corresponding author.
E-mail address: hhagino@jari.or.jp (H. Hagino).

http://dx.doi.org/10.1016/j.atmosenv.2016.02.014

motor vehicles. Specifically, brake wear particles are estimated to contribute 16–55% of non-exhaust traffic-related PM_{10} (particles up to 10 μm in size, which pertain to the 50% cut-off aerodynamic diameter) emissions (Harrison et al., 2013; Lawrence et al., 2013). Temporal patterns of brake wear particles in $PM_{2.5}$ emissions have been shown to exhibit periodic behavior, with two peaks coinciding with rush-hour traffic in street canyon traffic road tests and at an urban background site (Dall'Osto et al., 2013). Considering the increasingly strict controls on vehicle exhaust emissions, the relative contribution of brake wear particles will become increasingly important in the consideration of total traffic-related PM emissions (van der Gon et al., 2013). Furthermore, several toxicological studies have suggested that metallic brake wear particles damage tight junctions within the mechanisms that involve oxidative stress (Gasser et al., 2009; Zhao et al., 2015); therefore, the important point is not only the particle mass, but also the particle quality (e.g. chemical composition and biological effect).

The emissions and compositions of brake wear particles vary depending on a number of factors: (a) brake friction material parameters, for example, the contents of non-asbestos organics (NAOs), low-alloy steel, semi-metallic components, carbon composites, and rotor and drum parts (Garg et al., 2000; Sanders et al., 2003); (b) brake assembly type, including discs, drums, assembly sizes, surface structures, and depth of grooves (Garg et al., 2000); and (c) vehicle operating conditions, including initial speed, deceleration, pressure, torque, and brake temperature (Garg et al., 2000; Iijima et al., 2007, 2008; Sanders et al., 2003). Several studies have shown that airborne brake wear particles often differ considerably from the bulk friction material (Kukutschová et al., 2011; Österle et al., 2001). Studies into the mass balance measurement of airborne brake wear particles following braking events have estimated that 30–50% of generated brake wear debris becomes airborne (Garg et al., 2000; Sanders et al., 2003). The remaining brake wear particles are deposited on friction surfaces or attracted to other parts of the vehicle. It is also thought that brake wear substances can be generated from hydrocarbons derived from the gasification of resins in NAO friction materials (Garg et al., 2000; Inoue et al., 1990a, 1990b; Sanders et al., 2003) and/or from metallic components that decompose under tribo-reduction, which is defined as the reduction of metal oxides associated with friction (Okayama et al., 2013; Varrica et al., 2013). Additionally, there is also tribo-oxidation of metallic components (e.g., steel fibers, copper fragments) and oxidation of the rotor/disc (Hinrichs et al., 2011). While the quantity of emitted brake wear particles changes depending on the history of deceleration and acceleration under more realistic driving cycles (Hagino et al., 2015), current brake wear particle mass emission studies are typically performed according to initial speed/deceleration driving conditions and brake temperatures (Garg et al., 2000; Iijima et al., 2007, 2008). Vehicle exhaust emission-related PM has been studied and characterized in the laboratory using well-defined methods. However, brake wear particle emission measurements are both limited and complex, particularly because they involve both mechanical abrasion and the resuspension of wear particles deposited on brake friction surfaces. Therefore, further research is required to properly determine the emissions of brake wear particles, including the careful assessment of friction under transient driving cycles (Hagino et al., 2015).

However, using actual vehicles and/or roadway tests may result in PM samples that are contaminated by re-entrained road dust and/or tire wear particles (Sanders et al., 2003). To determine the emission factors and chemical compositions of brake wear particles from brake pads and rotors (or lining and drum) without contamination, which is important for toxicological testing of the particle-weighted emission factor (e.g., Cheung et al., 2009), it is better to use a brake wear particle dynamometer with an enclosing chamber and a constant-volume sampling system (Hagino et al., 2015). In this study, the emissions of airborne brake wear particles under transient driving cycles were measured using brake dynamometer measurements for commercially available automotive brake pads and lining assemblies. Furthermore, this study also examined the particle sizes and chemical compositions of the brake wear particles.

2. Experimental setup

2.1. Brake dynamometer

To facilitate the quantitative determination of airborne brake wear particle emissions, a chamber was placed around the brake assembly and a blower used to draw a constant flow of air past the brake assembly into the constant-volume sampling (CVS) tunnel (Fig. 1; Garg et al., 2000; Sanders et al., 2003; Iijima et al., 2007, 2008; Hagino et al., 2015). The equipment set-up was designed to allow for the use of two methods: one to determine the amount of wear on the brake pad/lining based on a test procedure using the inertia dynamometer (e.g., Japanese standard procedure for brake dynamometer testing of brake devices in passenger cars, JASO C427, which is essentially the same as BSL-035; Iijima et al., 2007), and the other based on an exhaust emission/fuel economy test procedure using a CVS tunnel (i.e., the Japanese Industrial Safety and Health Association (JISHA) Technical Standards (TRIAS) Attachment 42). Additional details are described in the Supporting Information (see "Brake Dynamometer") and elsewhere (Hagino et al., 2015).

2.2. Operating conditions

Three types of commercially available brake assemblies were used for the friction tests. According to a 2005–2010 survey of the Japanese vehicle market, these three manufacturers encompassed approximately 73% of passenger cars and 30% of trucks on the Japanese market. Two passenger cars (vehicles I and II) were selected for the analysis of the disc brake systems, and a middle-class truck (GVW8t class, vehicle III) was selected for the analysis of the drum brake systems (Table S1). Before the friction tests, the friction surfaces were burnished to remove roughness. Further details of the pre-conditioning are described in the Supporting Information (see "Operating Conditions").

The brake wear particle emission tests simulated driving on an urban road (Garg et al., 2000). Our preliminary work showed the importance of measuring brake wear particles emitted under a driving pattern that represents both deceleration and acceleration phases (Hagino et al., 2015). Therefore, measurements of airborne brake wear particles were attempted under transient driving cycles that represented such behavior. The brake assembly was set on the brake dynamometer and driven according to the Japanese JC08 transient emission test cycle (for gasoline powered passenger cars) or the Japanese JE05 transient emission test cycle (for diesel trucks; Rakopoulos and Giakoumis, 2009; Sekimoto et al., 2013). The JC08 and JE05 cycles consisted of many series of acceleration and deceleration phases that attempted to simulate driving on an urban road. During the final velocity plateau (i.e., the region with a maximum speed of 81.6 km/h for JC08 and 87.6 km/h for JE05), driving on a highway away from an urban environment was simulated. Fifty experiments for each brake assembly were performed by conducting ten tests per day over a five-day period. The braking frequencies and patterns of each vehicle were based on the actual traveling conditions of the vehicle. The test vehicles for each load weight condition were driven on a high-speed oval track (Fig. S1) and the braking patterns and brake temperatures were

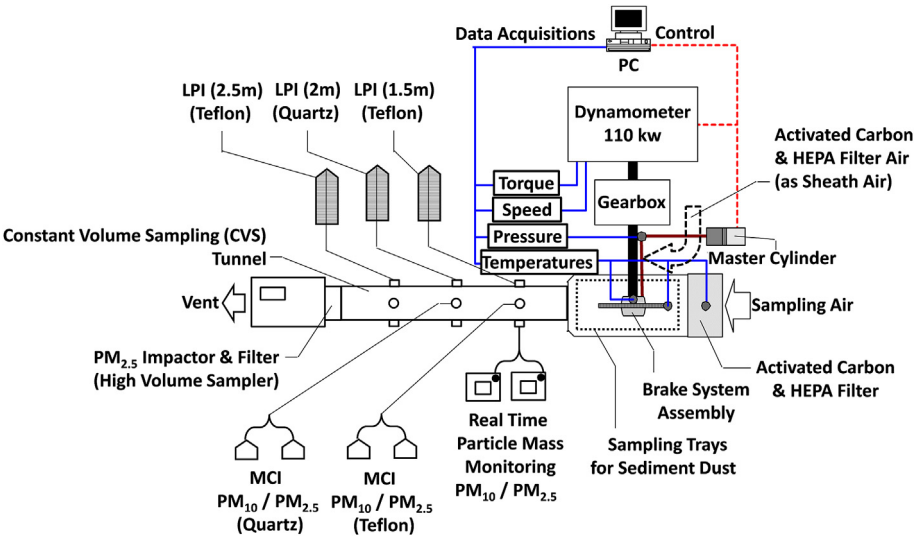

Fig. 1. Schematic of the brake dynamometer assembly and measurement instruments.

recorded. Consequently, the deceleration control responding to the behavior of the actual vehicle during the driving cycles was enabled, which corresponded to the driving operation performed by the driver at deceleration. Furthermore, the target driving torque of the dynamo-driven brake assembly was simulated and obtained by multiplying target total driving torque by the front/rear-braking force distribution (BFD) ratio (Iijima et al., 2007). Previous studies have indicated that brake temperature is an important parameter for brake wear particle emissions (Garg et al., 2000; Sanders et al., 2003; Iijima et al., 2007, 2008). The brake temperatures using the dynamometer experiment were not significantly different to those of an actual on-road vehicle test (see. 3.2 Mass Emissions).

2.3. Particulate matter collection and measurements

In most brake wear particle emission studies, brake dynamometer measurements with constant-volume sampling systems have focused exclusively on airborne PM emissions and the mass of wear of the pad and/or lining. The environmental impacts of brake wear particles originating from the fallout process have been discussed in relation to the sources of copper in the runoff (Armstrong, 1994) and in relation to particles resuspended from road surfaces (Harrison et al., 2013). Therefore, it is important to track the whereabouts of brake wear particles quantitatively in relation to the mass of wear of the brake discs or linings. Thus, in this study, three categories of emissions were measured by mass and by chemical analysis of inorganic elements: (a) fallout on the road (i.e., bottom of the chamber in this study); (b) deposition on the surfaces of the brake pads and linings; and (c) airborne PM. To estimate the amount of wear in the brake pads and linings quantitatively, the amount of Fe originating from the rotor or drum (Iijima et al., 2007) was subtracted from the three emission categories.

The PM fallout was collected on stainless steel trays placed on the bottom of the inside of the chamber. The PM deposited on friction materials was collected after the completion of the dynamo test schedule using a micro spoon-shaped spatula and brush apparatus. To quantify the mass emission from the airborne brake wear particles, samples were collected using eight filter sampling systems (Fig. 1). Further details of the particle sampling are described in the Supporting Information (see "Particulate Matter Collection and Measurements").

Real-time particle mass concentrations were measured by two particle mass monitors (DustTrakII™, TSI Inc.) with temporal resolutions of 1 s, which were equipped with PM_{10} and $PM_{2.5}$ impactors. After the driving operation, the values measured by DustTrak™ were corrected by the filter mass concentrations for each brake assembly test. The inlets were situated in the sampling tunnel at 1.5 m from the driving shaft, at the center of the automotive brake system.

As the airflow rate in the sampling tunnel was constant and the particle mass concentration was uniform for the tunnel cross section and distance (Hagino et al., 2015), the mass emission factor of the wheel was estimated as follows:

$$EF_{wheel} = C_{tunnel} \times V_{tunnel} \times t_{test}/D_{distance} \quad (1)$$

where EF_{wheel} is a PM mass emission factor for a wheel (mg/km/wheel) with the braking force distribution of the vehicle, C_{tunnel} is the PM mass concentration in the tunnel (mg/m^3), V_{tunnel} is the airflow rate in the tunnel (m^3/min), t_{test} is the time of a test cycle (min), and $D_{distance}$ is the driving distance of a test cycle (km).

The emission factor per vehicle $EF_{vehicle}$ (mg/km/vehicle) was estimated as follows:

$$EF_{vehicle} = EF_{wheel} \times N_{front} + EF_{wheel} \times N_{rear} \times BFD_{rear}/BFD_{front} \quad (2)$$

$$BFD_{rear} = 1 - BFD_{front} \quad (3)$$

where N_{front} and N_{rear} are the number of wheels on the front and rear of a vehicle, respectively, BFD_{front} and BFD_{rear} are the braking force distribution ratio of the front and rear wheels of the vehicle. As ideal braking force distributions are designed based on specific brake data (e.g., the effective diameter of a brake disc, brake drum, and the brake hydraulic pressure control device), the braking force distributions used followed the values proposed by each vehicle manufacturer. However, the actual brake force distributions varied (i.e., 0.6–0.8) during braking as a function of deceleration and initial speed (and gross vehicle weight). In other words, the braking force of each wheel changed according to the static load, which was caused by the shifting of the load by the inertial force during braking. In this study, the emission factors per wheel EF_{wheel} were measured under the only BFD_{front} condition and have the presumption of using the scale linearly with BFD. Therefore, it is

necessary to note that the brake wear particle mass emissions estimated by equation (2) are simplified.

2.4. Chemical analyses

Samples collected from Teflon® filters on the MCI (47 mmϕ) and LPI (80 mmϕ) were used to determine the concentrations of several inorganic elements using inductivity coupled plasma–mass spectrometry (ICP–MS). The preparation of the Teflon® filter media was conducted by microwave-assisted mixed acid (4.5 mL HNO_3, 0.5 mL HF, 1.3 mL HCl) digestion and then processed according to a Standard Operating Procedure (SOP; California Environmental Protection Agency Air Resources Board, 2010). In total, 17 elements (Na, Al, K, Ca, Ti, V, Cr, Mg, Mn, Fe, Cu, Zn, Sr, Zr, Mo, Sb, and Ba) were determined by ICP–MS (ICP–MS, 7500cx, Agilent Technologies Inc.). The analytical procedures were validated using several standard reference materials (SRMs; Table S2). The results showed that the analytical procedures for acid digestion and ICP–MS analysis had low interference with the target species. However, the acid digestion efficiencies for Ca were observed to be slightly lower, while those of the other 16 elements were consistent with certificated values.

The quantities of organic carbon (OC) and elemental carbon (EC) on the quartz substrates were determined using a thermal-optical carbon analyzer (Model 2001, Desert Research Institute), and the samples were processed according to the IMPROVE Thermal Desorption/Optical Reflectance method with a 550 °C split for OC and EC. Carbonaceous components in brake NAO friction materials include phenol resin, aramid fiber, natural rubber, graphite, and cashew dust (Chan and Stachowiak, 2004). The OC and EC in the brake wear particles were separated before being used for radiocarbon (^{14}C) measurements in order to distinguish fossil and contemporary carbon materials. Specifically, the ^{14}C measurements were conducted on total carbon (TC) and EC samples for each test using acceleration mass spectrometry (Paleo Laboratory, Ltd.; Minoura et al., 2012). The EC samples were prepared with an aqueous extraction and heated at 550 °C to remove OC (Gelencsér et al., 2010). High-resolution flight aerosol mass spectrometry (ToF-AMS, Aerodyne Research, Inc.) with electron ionization (EI) was also employed in the analysis of the organic component for vehicle II (temporal resolution of 1 s), because it was associated with the highest PM concentrations observed in this study. Further details of the chemical analyses are described in the Supporting Information (see "Chemical Analyses").

3. Results and discussion

3.1. Time series mass emissions

To the best of our knowledge, time-resolved measurements of airborne brake wear particles have never been performed during transient driving cycles representing both acceleration and deceleration phases. To study brake wear particle emissions as a function of vehicle operating conditions and cycles, instruments with a time resolution of the order of 1 s are needed. Therefore, in this study, two disc brake systems (for passenger cars) and a drum brake system (for trucks) were investigated in order to determine time series variations in $PM_{2.5}$ and PM_{10} mass emissions during JC08 (disc brakes) and JE05 (drum brakes) cycles using two light-scattering laser photometers (DustTrak™).

Fig. 2a–c shows an example time series for vehicle speed and mass concentrations (mg/s/wheel) of PM_{10} and $PM_{2.5}$ during typical JC08 and JE05 test cycle experiments (runs #1 and #10). Run #1 for each vehicle corresponded to a cold start for the exhaust test, which resulted in lower PM emissions compared with run #10, which corresponded to a hot start. There were no significant differences in the peak emission patterns, and large peaks of brake wear particles appeared during the highway-driving mode between 1040 and 1230 s for JC08, and between 1410 and 1840 s for JE05. However, the details of the emission patterns varied between different brake assemblies. The time-resolved emission profiles for PM_{10} and $PM_{2.5}$ were similar, particularly for vehicle III, which had almost similar levels of PM_{10} and $PM_{2.5}$ emissions. This suggests that both fine particles (<2.5 μm) and coarse particles (2.5–10 μm) significant components of break wear particles (see Section 3.2).

The time series pattern of vehicle I was roughly similar to vehicle II. Two peak types were found, one during the application of a braking force and one during wheel rotation. The first was obtained during a braking event (Fig. 2) and indicated that brake wear particles were derived from the collision and friction between the disc and the pads. The second type was obtained during a rotor rotation and acceleration event (Fig. 2), and these data suggest that brake wear particles can also be derived from the detachment of wear particles from the surface of the brake and grooves. This was probably caused by the use of a disc brake assembly with an open (not sealed) configuration (Iijima et al., 2008). Another reason was probably the design of the disc brakes, where the brake pad might remain in contact with the disc even when the brakes are no longer applied (i.e., "drag"). Drag occurs because there is no mechanism that actively draws the pads away from the discs after braking (Backstrom, 2015). However, in our findings there was no rise in brake temperature during the acceleration phase; therefore, it was difficult to judge if contact occurred between the pads and rotor (Fig. S2a–c). Furthermore, the disengagement of the brake pad could be confirmed by the naked eye by looking through the observation window on top of our brake dynamometer chamber (Fig. S4). There is no conclusive evidence that the emissions of brake wear particles occurs following the slightest touch during driving, and further investigation into this was beyond the scope of this study. Therefore, we concluded that under the present experimental conditions, the emission of brake wear particles during driving was not negligible.

For the drum brake (Fig. 2c), only one type of peak was found when applying a braking force. The peak increment started with the application of the braking force (Fig. 2) and there may have been slight emissions during driving with a rotating rotor. The drum brake assembly is a closed system with a drum and back plate, and the clearance gap is less than 1 cm, which suggests that the brake wear particles are largely retained inside the drum and rarely emitted to the outside environment (Hagino et al., 2015). Previous studies have shown that, in contrast to disc brake systems, drum brake system emissions correspond to a low percentage of the total wear particles (Garg et al., 2000; Iijima et al., 2007; Hagino et al., 2015). While these studies are not directly comparable to ours, they do support the differences observed between the open and closed brake assemblies. The results of this study also show that brake wear particles can be released by brake abrasion and the swirling airflow resulting from the rotor or drum after a braking event. The contribution of resuspended particle emissions during driving is consistent with our preliminary study (Hagino et al., 2015).

3.2. Mass emissions

The brake wear particle (PM_{10} and $PM_{2.5}$) emission factors were compared with run number and brake temperature (Fig. S2). PM mass emissions varied with run number, and those of vehicles II and III increased with run number. As emission tests were performed 10 times per day, the first run corresponded to a cold start that resulted in lower brake temperatures and PM emissions. Pad

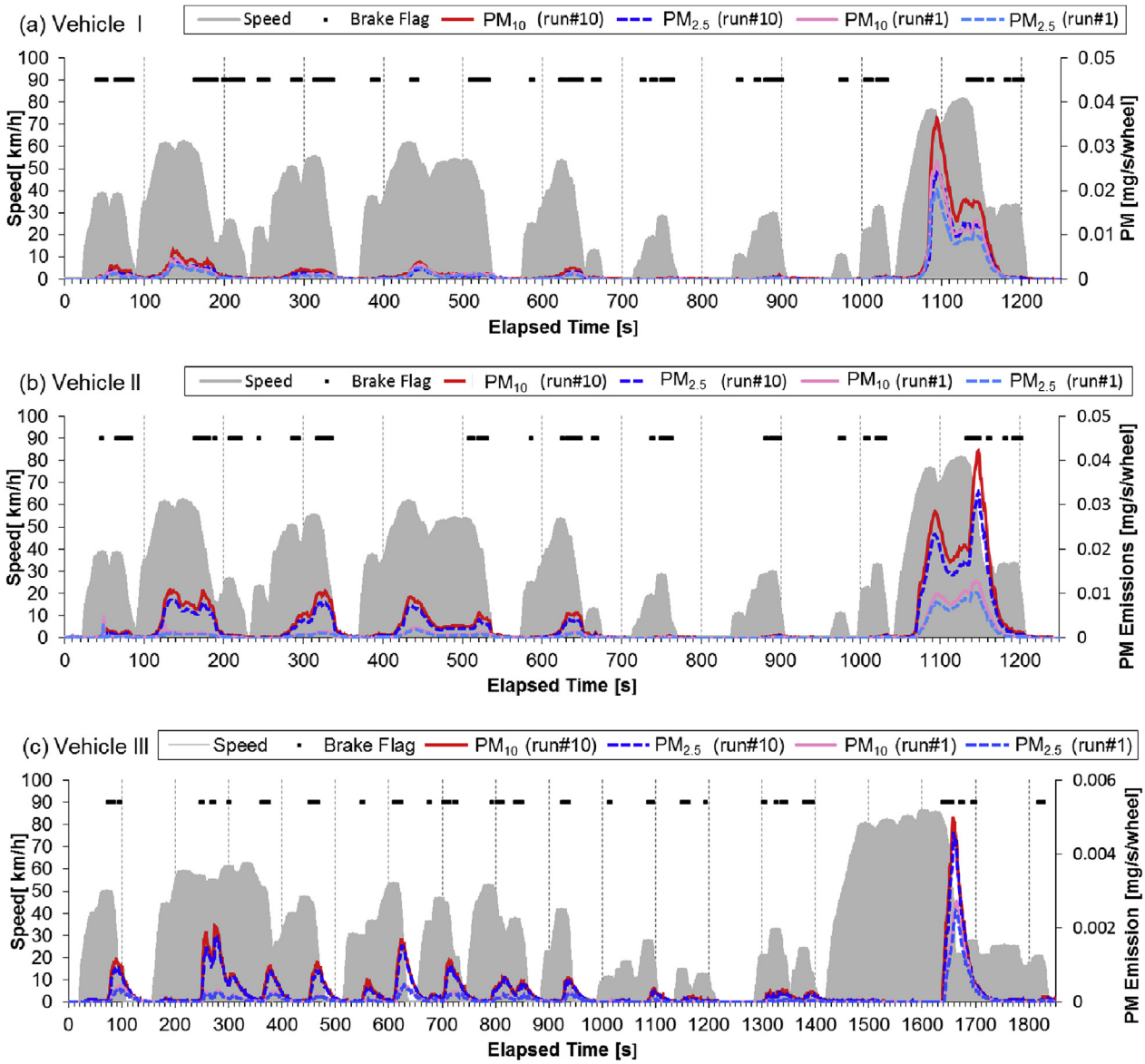

Fig. 2. Time series profiles of brake wear particle mass emissions of PM_{10} (red line = run #10/pink line = run #1) and $PM_{2.5}$ (dashed dark blue line = run #10/dashed light blue line = run #1) during transient driving test cycles: (a) vehicle I; (b) vehicle II; and (c) vehicle III. Grey shading denotes vehicle speed and black squares denote braking flags. (For interpretation of the references to colour in this figure legend, the reader is referred to the web version of this article.)

wear rate is approximately proportional to the initial velocity squared at temperatures of 50–300 °C (Zhang et al., 2009), which suggests that the brake wear particle emissions in this study were sensitive to brake temperature (Kukutschová et al., 2011). In other words, brake temperature control is an important parameter that must be considered when measuring brake wear particle emission factors, and test methods for the acquisition of representative values should be within the normal range of temperatures (100–200 °C; Garg et al., 2000) generated during normal brake use. The brake temperature ranges (maximum during a cycle) in this experiment were 101–142 °C (vehicle I), 72–94 °C (vehicle II), and 87–135 °C (vehicle III). Thus, these temperature data are in the valid temperature range and comparable with practical data from actual test vehicles. When brakes were tested at each load weight condition on a high-speed oval track under the same transient driving cycles, but with 5 repeat tests involving 10-min intervals, the brake temperature ranges (maximum during a cycle) were 102–113 °C, 72–74 °C, and 97–133 °C for vehicles I, II, and III, respectively.

Using light-scattering laser photometry, the mean mass emission factors of PM_{10} and $PM_{2.5}$ for the filter data were estimated to be 0.67 and 0.53 mg/km/vehicle (ranges of 0.58–1.00 and 0.39–0.76 mg/km/vehicle), respectively, for vehicle I. For vehicle II they were 1.38 and 1.00 mg/km/vehicle (ranges of 0.39–1.44 and 0.31–1.21 mg/km/vehicle), respectively, and for vehicle III, they were 0.16 and 0.11 mg/km/vehicle (ranges of 0.04–0.16 and 0.04–0.15 mg/km/vehicle), respectively. We also found that the NAO brake wear particle emissions varied with brake assembly type. In particular, the drum brake assembly with a closed system emitted less brake wear particles than the open disc brake assembly, consistent with the results of our preliminary study. Incidentally, the estimated brake wear particle mass emissions were simplified using a single wheel (a front brake assembly) test and braking force distribution as above. Based on a previous study and our findings, contributions from resuspended particles due to wheel-induced turbulence should be noted, and will require large-

scale reconstruction of the existing equipment (Sanders et al., 2003; Hagino et al., 2015). For this reason, we also tried a calculation based simply on single wheel emission (EF_{wheel}) estimations multiplied by the number of wheels (N_{wheel}) using Eq. (2). The averaged mass emission factors of PM_{10} and $PM_{2.5}$ for the filter data were mostly estimated to be 0.94 and 0.74 mg/km/vehicle, respectively, for vehicle I, and 1.93 and 1.40 mg/km/vehicle, respectively, for vehicle II. For vehicle III, there was no difference in the emission values because the braking force distribution used the same value (0.5) between the front and rear brakes.

Previous studies have determined emission factors for brake wear using several methods. First, direct measurements have been conducted with dynamometers during laboratory experiments or with vehicles during road tests. Second, receptor modeling has been applied for field measurements under certain environmental conditions. With regard to direct measurements, brake dynamometers with isokinetic sampling systems have been used in several studies for estimating brake wear emission factors for light-duty vehicles (LDVs), and these studies yielded values in the range of 3.0–8.0 mg/km/vehicle (PM_{10}) and 2.1–5.5 mg/km/vehicle ($PM_{2.5}$; Grigoratos and Martini, 2014). With regard to receptor modeling, several receptor models have been applied in different environments (e.g., tunnels, street canyons, or roadside environments) to estimate brake wear emission factors for LDVs, and these studies yielded values in the range of 1.0–8.8 mg/km/vehicle (PM_{10}), depending on the observation site (Grigoratos and Martini, 2014). The brake wear particle emissions in this study were found to be slightly lower than the values reported in previous studies; however, reasonable emission levels for inorganic elements were obtained when the results of this well-controlled conditional experiment and real-world emission measurements were compared (e.g., Sb; see section 3.6 Inorganic Elements). Moreover, the brake wear particle mass emission factors displayed large variations depending on brake material, assembly system, and environmental conditions. Further measurements under a wide range of driving conditions will be required to characterize the emissions of brake abrasion dust properly, and these should be obtained by carefully assessing friction under transient driving cycles.

3.3. Size distributions

Fig. 3 shows the particle mass size distributions of emissions from the three vehicles under the transient driving cycle tests. The distributions from these three vehicles were dominated by the <10 μm range, with a unimodal shape mass size range of 0.68–3.5 μm; however, in contrast to a previous study using an NAO disc (Garg et al., 2000), there was no significant contribution from ultrafine particles (<0.1 μm). Vehicles I and II (disc brakes) show similar distributions with a peak in the 1.2–3.5-μm range, but vehicle III with the drum brake had a greater quantity of smaller-sized particles (1.2–2 μm). This difference in the size distribution reflects differences in the brake assembly structure between the disc and drum systems. The drum brake assembly is a closed system with a drum and back plate and a sub-centimeter clearance gap; thus, the brake wear particles can be retained within the drum, becoming fractionated according to particle size. For an open (not sealed) disc brake assembly, coarse and fine particles of brake wear dust may be emitted because there is no sieving mechanism. Time series profiles obtained in a previous study differed between disc and drum brakes (Hagino et al., 2015), and though those results may not be directly comparable with our study, they support the differences observed between the open and closed brake assemblies.

Using an enclosed chamber, some previous studies (Garg et al., 2000; Iijima et al., 2007) have examined the mass size distributions of brake wear particles for several kinds of brake assemblies and temperature conditions. Their results suggested that variations in dust emissions might be caused mainly by differences in braking temperatures and pad types; the brake wear particle emissions reported for NAO brakes were in size ranges of 0.1–1.0 μm (Garg et al., 2000) and 3–6 μm (Iijima et al., 2007). Based on a comparison of dust emissions using two LPI samples in the 0.68–3.5-μm range, the variations of mass size reported as relative standard deviations were 3.8–10% (vehicle I), 0.5–20% (vehicle II), and 0.4–2.7% (vehicle III), indicating that particle losses in the sampling tunnel were not significant. Even though the same NAO-type pads were used in these previous studies, it is interesting to note that dust emission values exhibited large variations. The variations in size distribution might also be caused by differences in braking conditions and friction varieties, as suggested in previous studies (Hagino et al., 2015); thus, further friction studies are recommended.

The mass fractions of $PM_{2.5}$ and PM_{10} in the MCI sampler, and that of fine particles (≤2.1 μm) to coarse particles (3.5–11 μm of the LPI sampler were 79% and 49% (vehicle I), 72% and 55% (vehicle II), and 69% and 68% (vehicle III), respectively (Table S3). The systematic bias for the emission of fine particles, detected by the two different sampling methods, also showed in the standard deviations, which were 32% (vehicle I), 21% (vehicle II), and 2% (vehicle III). As brake wear particles from drum brakes are smaller than those from disc brakes (Fig. 3), drum brakes show lower variations in mass size distributions in the different sampling methods. Emissions of inorganic elements from the vehicles showed similar size distributions as the PM mass emissions, consistent with their friction materials (see Section 3.6). However, the difference between the PM and the element size distribution might be caused by the unexpected acid digestion error for the vehicle I filter.

3.4. Mass balance

Fig. 4 shows the brake wear particle masses of the three vehicles during the 50 transient driving cycle tests. The Fe from the rotor or drum were subtracted from the emissions, because brake wear particles can include those originating from the friction pair (rotor or drum; Iijima et al., 2008). Cast iron in the friction pairs was assumed to be 100% Fe and this was used as an indicator of friction pair wear (Iijima et al., 2008). Considering that the mass percentages of Fe in the pads and linings accounted for 0% (vehicle I), 0.35% (vehicle II), and 0.05% (vehicle III), the contribution of Fe in the PM was taken to come from the disc or drum, while the contribution of Fe from the pads or linings was considered to be negligible. The masses of emissions based on the amount of abrasive wear per driving distance were 6.3, 4.7, and 5.8 mg/km/vehicle for vehicles I, II, and III, respectively (Table S4). The percentage of the total wear detected as total airborne PM and $PM_{2.5}$ accounted for 13% and 8% (vehicle I), 29% and 21% (vehicle II), and 4% and 2% (vehicle III), respectively. Not all brake wear particles were emitted as airborne particles and the mass of wear particles did not correspond to the airborne PM emissions. This is consistent with previous studies, which have shown that not all brake wear particles are emitted as airborne particles, and that 30–90% of brake wear particles by mass are emitted as airborne PM (Garg et al., 2000; Sanders et al., 2003; Iijima et al., 2008).

It was found that a portion of the brake wear particles remained on the surface of the brakes and grooves: 0.04% for vehicle I, 5% for vehicle II, and 51% for vehicle III. The shoe (drum brake) had some drill holes for the rivet or bolt fastenings, which increased the percentage of wear particles deposited on the shoe (Table S1). The unaccounted mass fractions contributed significantly to the mass of

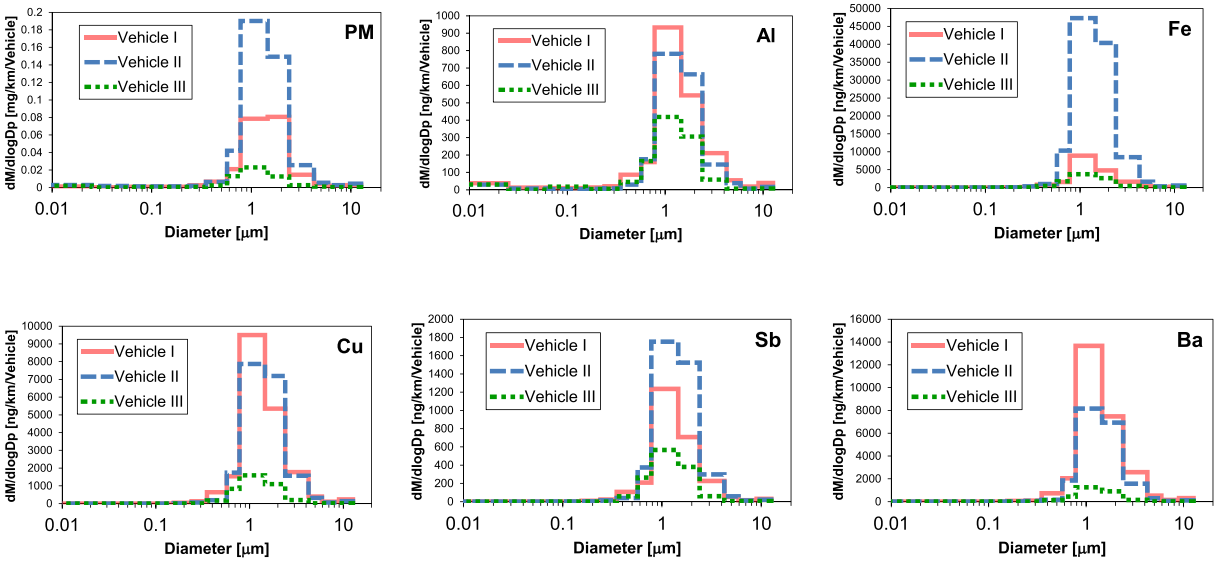

Fig. 3. Size-resolved particle mass and inorganic element emissions obtained during transient driving test cycles for vehicles I (pink lines), II (blue lines), and III (green lines). Data were analyzed by ICP–MS. Samples were collected using 12-stage LPI samplers. (For interpretation of the references to colour in this figure legend, the reader is referred to the web version of this article.)

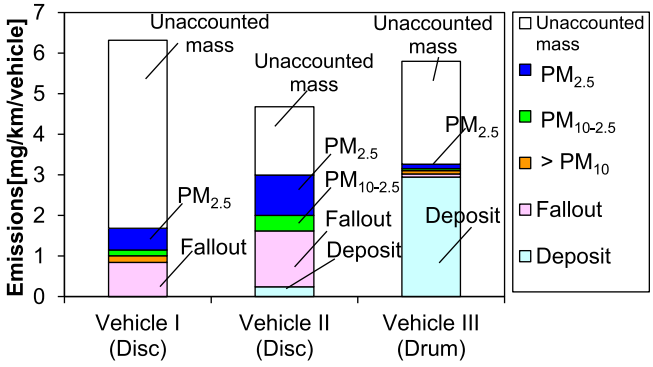

Fig. 4. Wear mass balance obtained during transient driving test cycles for vehicles I, II, and III. The Fe contents originating from the rotor and drum were subtracted from these data.

the wear, accounting for 73%, 36%, and 44% for vehicles I, II, and III, respectively. The reasons for this were probably errors in collection and measurement (i.e., the fallout, deposit, and weighing of the brake assemblies) or the release of gaseous species from the friction materials. A 25% error in the weight of the disc and lining by the microbalance would result in significant unaccounted fractions, accounting for 59–98%, 29–48%, and 35–58% for vehicles I, II, and III, respectively. Based on the results of previous studies (Inoue et al., 1990a, 1990b) and on the carbon component measurements (see Section 3.5), it appears that there is a mechanism of gaseous species emission or chemical change in NOA friction during the abrasion process, and the same explanation may apply for this case.

Gaseous species emissions reported by a previous study showed a consistent pattern of HC emissions synchronized with braking events (Garg et al., 2000). It is well known that NAO brake pads (discs) and shoes (drums) contain metal and organic components that prevent the lowering of the coefficient of friction during the decomposition of organics. This decomposition (oxidation), known as the mechanochemical degradation of cured resin, is due to the increase in temperature caused by the shearing forces. It has been reported that metal powder can decrease the average molecular weight of the degradation products of phenolic resin (e.g., CO_2, CO, aldehydes, and aromatics) through catalytic action (Inoue et al., 1990a, 1990b). Moreover, reduction of metal oxides associated with the tribo-degradation of phenolic resin (e.g., $CuO \rightarrow Cu + O$) has also been reported (Okayama et al., 2013). Another study indicated that Sb_2S_3 in lubricants (Varrica et al., 2013; Chan and Stachowiak, 2004) decomposes to more stable mixed oxidized forms (e.g., Sb_2O_3) through the brake abrasion process (Varrica et al., 2013), corresponding to the loss or transformation of sulfur. Measurement of the carbon content of no-airborne low-metallic brake debris from friction tests indicated that the original brake pad sample contained 494 g/kg of carbon (56 wt% for the pad), which fell to 141 g/kg in the wear debris sample (40 wt% less than the original pad) after the friction test (Plachá et al., 2016). Therefore, the unaccounted fraction may reflect gasification, including oxidation, reduction and evaporation from brake friction. Although neither this nor the previous study quantified gaseous substances, this finding is a tentative insight into the brake abrasion mechanism. In future, better measurements will be required to determine gaseous species (i.e., CO_2 and hydrocarbons) emissions at lower temperatures, or to better quantify their fractional contribution to the mass of wear.

3.5. Carbon components

The TC emissions of PM_{10} and $PM_{2.5}$ accounted for 71 μgC/km and 67 μgC/km/vehicle, respectively, for vehicle I, 110 μgC/km/vehicle and 83 μgC/km/vehicle, respectively, for vehicle II, and 66 μgC/km/vehicle, and 63 μgC/km/vehicle, respectively, for vehicle III (Table S5). The TC contributions of PM_{10} and $PM_{2.5}$ accounted for 7.3% and 13%, respectively, for vehicle I, 7.9% and 8.3%, respectively, for vehicle II, and 41% and 57%, respectively, for vehicle III. The TC of airborne PM from the disc brake was found to have lower percentages than the 21% and 17% reported for 100 °C and 300 °C tests (Garg et al., 2000), indicating variations in the amount and ratio of TC from PM caused by differences in brake friction and temperature. For reference, the carbon contents of the pads and linings were semi-quantified as 37%, 34%, and 64%, for vehicles I, II, and III, respectively (Fig. S3a), suggesting that parts of the carbon

components were volatilized and/or oxidized. The carbon component loss from PM_{10} during friction accounted for 25%, 26%, and 22% (9%, 9%, and 14% of total mass) for vehicles I, II, and III, respectively. The permutable ranges detected for the unaccounted fraction of the wear of the mass were 73%, 36%, and 44% for vehicles I, II, and III, respectively (Fig. 4).

As carbonaceous components from NAO brake friction are included in phenol resin, aramid fiber, natural rubber, and cashew dust (Chan and Stachowiak, 2004), the contemporary carbon content (pMC) was determined for subsequent radiocarbon (^{14}C) measurements (see Supporting Information "Chemical Analyses"). The pMC of TC from the original friction materials (pad and lining), and from airborne $PM_{2.5}$ brake wear particles generated by the abrasion process, accounted for 28.7 and 20.1, respectively, for vehicle I, 20.1 and 11.6, respectively, for vehicle II, and 10.1 and 13.2, respectively, for vehicle III. The pMC in this study was lower than the value of 51 (Hildemann et al., 1994). This reflects the wide variations in pMC caused by differences in brake friction. On the other hand, under a shearing force from the mechanochemical degradation process, the metal powder in cured phenolic resin has been found to decrease the mean molecular weight of the degradation products through catalytic action (Inoue et al., 1990a, 1990b). These studies cannot be directly compared with our study; however, they might support the change of large molecular weight carbon components, which can be volatilized or oxidized to CO_2, causing large alterations in chemical compositions. In any case, it remains difficult to spectate over which substances are combustible during the mechanochemical reaction; therefore, this study presents the experimental data as a case study only.

Organic and sulfur components were found in the non-refractory submicron particle phase (NP-PM_1) using a Time-of-Flight Aerosol Mass Spectrometer (ToF-AMS) under normal in-use 600 °C detection (Fig. 5), indicating that they originated from organics in the NAO friction materials, barium sulfate, and antimony pentasulfide. The O/C and H/C ratios of the organic compounds were 0.68 and 1.62, respectively. Although the organics from brake wear particles were primary organic aerosols (POAs), higher oxidative components we also observed, in contrast with the NAO brake materials (e.g., O/C 0.11 and H/C 1 for a monomer phenol resin and O/C 0.14, and H/C 0.57 for a monomer aramid fiber; Chan and Stachowiak, 2004) and tailpipe emissions (e.g., O/C/0.03 and H/C 2 for gasoline and diesel exhausts; Mohr et al., 2009). There were similar oxidation levels for secondary organic aerosols (SOAs; e.g., O/C 0.68 and H/C 1.27 for toluene-derived SOAs; Chhabra et al., 2010) and ambient water soluble organic aerosols as oxygenated components (e.g., O/C 0.64 and H/C 1.45; Mihara and Mochida, 2011). These results indicate that the NAO friction particles changed to oxygenated organic particles during the abrasion process.

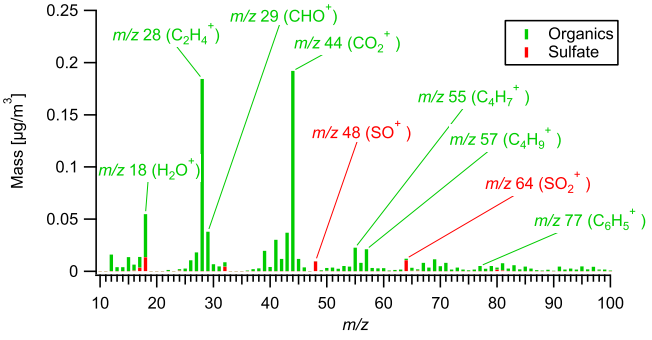

Fig. 5. Average aerosol mass spectra of organic (green) and sulfate (red) brake dust emissions for vehicle II. (For interpretation of the references to colour in this figure legend, the reader is referred to the web version of this article.)

3.6. Inorganic elements

Fig. 3 shows the size distributions of brake wear particle emissions for typical inorganic elements (Fe, Cu, Sb, and Ba) measured during a dynamometer test, other inorganic elements (Ca, Sr, Cu, Mg, Sr, Na, Zn, Mo, K, Ti, and Zr) are shown in Fig. S7. The inorganic elements showed size distributions similar to those of the PM emissions, consistent with a unimodal mode (1.25–3.2 μm). In contrast to the mode size found in this study (~1–3 μm size distributions of the key tracer elements (e.g., Cu, Sb, and Ba; Grigoratos and Martini, 2014) showed a unimodal size distribution (≤2–5 μm) in a brake dynamo test (Iijima et al., 2007) and in a road tunnel (Lough et al., 2005), with these elements being significant relative to the effect of resuspension in tunnels. However, differences in size distributions often appear in other studies (e.g., mass size range of the <0.1 μm ultrafine mode; Garg et al., 2000), and it is interesting to note that size distributions show large variations due to differences in brake pads and/or sampling sites (Grigoratos and Martini, 2014). Moreover, previous studies have indicated that the emission of brake wear nanoparticles (and not accumulation mode particles) by number concentration increases above critical temperatures (i.e., 170–180 °C), and dominate at temperatures exceeding 200 °C. The same explanation may apply to results of this study (Oleksii et al., 2015).

The inorganic element emission factors from the MCI are shown in Table S5, together with values from the dynamometer, road tunnel, and tailpipe emissions tests of previous studies. In this study, the most abundant inorganic element in the brake wear particles was Fe and its fractions of PM_{10} and $PM_{2.5}$ were 12% and 10%, respectively, for vehicle I, 26% and 28%, respectively, for vehicle II, and 22% and 21%, respectively, for vehicle III (Table S6). Fe contents vary in the pads and linings of passenger cars (equivalent to vehicle I), compact cars (equivalent to vehicle II), and trucks (equivalent to vehicle III; Fig. S6b). The mass fractions of brake wear particles originating from rotors have been estimated to be ≤30% (Iijima et al., 2008). In this study, the mass fractions of PM_{10} and $PM_{2.5}$ brake wear particles originating from the rotor or drum accounted for 22% and 20%, respectively, for vehicle I, 19% and 20%, respectively, for vehicle II, and 10% and 9%, respectively, for vehicle III (Table S6). This shows that the contributions from the rotor or drum in this study were similar to those in the previous NAO brake pad study (Iijima et al., 2013); however, this applies only to NAO linings. For semimetallic or metallic linings, the Fe content in PM is partially due to the pad/lining and not only to the disc/rotor.

Brake wear particles were measured as a driving distance-based mass emission; therefore, the emission factors of the inorganic elements can be compared with those from tunnel environments or tailpipe emission tests. The key tracers of brake wear particles (Grigoratos and Martini, 2014) varied by vehicle (i.e., by brake assembly) for $PM_{2.5}$, with ranges of 2.4–5.5 (Al), 0.51–2.1 (Ca), 23–277 (Fe), 8.1–55 (Cu), 2.6–9.7 (Sb), and 7.1–81 (Ba) μg/km/vehicle (Table SX). These elements are included in almost all pads and linings; however, the fractions vary widely (Fig. S6b). Tailpipe emissions tend to have a higher range of OC, EC, Ca, and K than brake wear particle emissions, suggesting that these elements originate from engine lubricant. The OC, EC, Al, Ca, and K of road tunnel emissions have higher levels than brake wear particles, suggesting that tailpipe emissions and resuspended particles contribute more to PM emissions than brake wear particles. The concentrations of Zn and Cu in brake wear particles and road tunnels were similar; however, Ba contents were higher in brake wear particles than in tailpipe emissions.

The emission factors of Sb, a typical tracer used as a solid lubricant in brake pad/linings (Chan and Stachowiak, 2004), determined in previous studies were 4–18 (light duty vehicles) and 44–128 μg/km/vehicle (heavy duty vehicles) for an inter-urban freeway with free-flowing traffic, 144 μg/km/vehicle for a street canyon in Stockholm (Johansson et al., 2009), 32 μg/km/vehicle for Tingstad tunnel in Sweden (Sternbeck et al., 2002), 51 μg/km/vehicle for Lundby tunnel in Sweden (Sternbeck et al., 2002), 16 μg/km/vehicle for Kilborn tunnel in the United States (Lough et al., 2005), and 12–67 μg/km/vehicle for Howell tunnel in the United States (Lough et al., 2005); therefore, our results showed similar emission levels depending on brake type and sampling site. In other words, the results suggest that emissions in laboratory brake dynamometer test are capable of being detected in traffic-related ambient PM. Moreover, despite the small concentration of emitted Sb, high Sb levels in the blood of port workers (5–10 times higher than the concentration of Sb in the blood of control groups) suggest the significant impact of Sb emissions from heavy weight vehicle traffic (Quiroz et al., 2009). Therefore, even low-level emissions may be detectable in the atmosphere and impact upon human exposure.

A Cu/Sb ratio of 4.6 ± 2.3 has been proposed as typical for brake wear particles (Sternbeck et al., 2002). The mean value of our three vehicles' brake wear particle emissions showed a similar ratio (i.e., 5.6 ± 2.6). However, it is interesting to note that large variations in this ratio due to variations in brake pad composition have been reported (Grigoratos and Martini, 2014). In the disc brakes used by several Japanese manufacturers (Fig. S6c), Sb was not detected in the brake pads, indicating that brake manufacturers may substitute Sb sulfides with Sn sulfides (SnS or SnS_2; Faullant, 2002). In addition, brake pads need to be compliant with state regulations, which stipulate that from the beginning of 2021, brake pads must have low Cu contents (Washington State Senate Bill SB6557, 2010; California State Senate Bill SB346, 2010; Lee et al., 2012). Thus, attention should be given to the Cu/Sb ratio, as this will change during source apportionment environmental analyses in future studies. Further research is required to determine the national and regional specific emission factors of brake abrasion dust and a greater number of friction materials should be assessed under transient driving cycles, similar to the tailpipe emission test method.

4. Conclusions

To determine the emission factors and chemical compositions of brake wear particles from brake pads and rotors (or lining and drum) without contamination from road dust and/or tire wear, laboratory-based brake dynamometer measurements were used to test commercially available automotive brake pads and lining assemblies. The major conclusions of this study can be summarized as follows:

- Time series patterns for the two vehicles with disc brakes were roughly similar, with two peak types found during the application of a braking force and wheel rotation.
- For the drum brake, a single peak type was found when applying a braking force. This likely reflects the closed system of the brake assembly, with a drum and back plate, meaning that few brake wear particles are emitted from the narrow clearance and most are retained inside the drum.
- The observed airborne brake wear particle emissions ranged from 0.04 to 1.4 mg/km/vehicle for PM_{10}, and from 0.04 to 1.2 mg/km/vehicle for $PM_{2.5}$.
- Not all brake wear particles were emitted as airborne particles and mass of wear particles did not correspond to airborne PM emissions. The proportion of brake wear debris collected as airborne brake wear particles was 2–21% of the mass of wear.
- Oxygenated carbonaceous components were observed in the airborne PM by AMS, which indicated that changes in the oxidation of carbonaceous compounds occurred during the abrasion process.
- This study identified key tracers of brake wear particles (e.g., Fe, Cu, Ba, and Sb) at emission levels comparable with traffic-related atmospheric environments (e.g., tunnels, street canyons, or roadside environments).

Acknowledgments

We gratefully thank our co-workers on the brake wear particle emissions measurement project (April 2010–March 2014) at the Japan Automobile Research Institute for their design, construction, and testing of the brake wear particle dynamometer. We also thank the editor and reviewers for their careful reading of our manuscript and for providing constructive comments.

Appendix A. Supplementary data

Supplementary data related to this article can be found at http://dx.doi.org/10.1016/j.atmosenv.2016.02.014.

References

Armstrong, L.J., 1994. Contribution of Heavy Metals to Storm Water from Automotive Disc Brake Pad Wear. Woodward-Clyde Consultants, Oakland CA. Submitted to the Santa Clara Valley Nonpoint Source Pollution Control Program.
Backstrom, A., 2015. Brake Drag Fundamentals. SAE Int. http://dx.doi.org/10.4271/2011-01-2377.
California Environmental Protection Agency Air Resources Board, 2010. Procedure for the Determination of Trace Elements in Particulate Matter Emitted from Motor Vehicle Exhaust Using Inductively Coupled Plasma Mass Spectrometer (ICP-MS). SOP No. MLD 152.
California State Senate Bill SB346, 2010. Hazardous Materials: Motor Vehicle Brake Friction Material.
Chan, D., Stachowiak, G.W., 2004. Review of automotive brake friction materials. Proc. Inst. Mech. Eng. Part D. J. Automob. Eng. 218, 953–966. http://dx.doi.org/10.1243/0954407041856773.
Cheung, K.L., Polidori, A., Ntziachristos, L., Tzamkiozis, T., Samaras, Z., Cassee, F.R., Gerlofs, M., Sioutas, C., 2009. Chemical characteristics and oxidative potential of particulate matter emissions from gasoline, diesel, and biodiesel cars. Environ. Sci. Technol. 43, 6334–6340. http://dx.doi.org/10.1021/es900819t.
Chhabra, P.S., Flagan, R.C., Seinfeld, J.H., 2010. Elemental analysis of chamber organic aerosol using an Aerodyne high-resolution aerosol mass spectrometer. Atmos. Chem. Phys. 10, 4111–4131. http://dx.doi.org/10.5194/acp-10-4111-2010.
Dall'Osto, M., Querol, X., Amato, F., Karanasiou, A., Lucarelli, F., Nava, S., Calzolai, G., Chiar, M., 2013. Hourly elemental concentrations in $PM_{2.5}$ aerosols sampled simultaneously at urban background and road site during SAPUSS–diurnal variations and PMF receptor modelling. Atmos. Chem. Phys. 13, 4375–4392. http://dx.doi.org/10.5194/acp-13-4375-2013.
Dockery, D.W., Pope III, C.A., 2006. Health effects of fine particulate air pollution: lines that connect. J. Air Waste Manage. Assoc. 56, 709–742. http://dx.doi.org/10.1080/10473289.2006.10464485.
Faullant, P., 2002. Particle Size Effects of Tin Sulfides in Disc Brake Pads. SAE Int. http://dx.doi.org/10.4271/2002-01-2591.
Garg, B.D., Cadle, S.H., Mulawa, P.A., Groblicki, P.J., 2000. Brake wear particulate matter emissions. Environ. Sci. Technol. 34, 4463–4469. http://dx.doi.org/10.1021/es001108h.
Gasser, M., Riediker, M., Mueller, L., Perrenoud, A., Blank, F., Gehr, P., Rothen-Rutishauser, B., 2009. Toxic effects of brake wear particles on epithelial lung cells in vitro. Part. Fibre Toxicol. 6, 1–13. http://dx.doi.org/10.1186/1743-8977-6-30.
Gelencsér, A., Hoffer, A., Molnár, A., Krivácsy, Z., Kiss, Gy, Mészáros, E., 2010. Thermal behavior of carbonaceous aerosol from a continental background site. Atmos. Environ. 34, 823–831. http://dx.doi.org/10.1016/S1352-2310(99)00206-X.
Grigoratos, T., Martini, G., 2014. Brake wear particle emissions: a review. Environ. Sci. Pollut. Res. Int. 22, 2491–2504. http://dx.doi.org/10.1007/s11356-014-3696-8.
Hagino, H., Oyama, M., Sasaki, S., 2015. Airborne brake wear particle emission due to braking and accelerating. Wear 334–335, 44–48. http://dx.doi.org/10.1016/j.wear.2015.04.012.
Harrison, R.M., Jones, A.M., Gietl, J., Yin, J., Green, D.C., 2013. Estimation of the contributions of brake wear particles, tire wear, and resuspension to non-

exhaust traffic particles derived from atmospheric measurements. Environ. Sci. Technol. 46, 6523–6529. http://dx.doi.org/10.1021/es300894r.
Hildemann, L.M., Klinedinst, D.B., Klouda, G.A., Currie, L.A., Cass, G.R., 1994. Sources of urban contemporary carbon aerosol. Environ. Sci. Technol. 28, 1565–1576. http://dx.doi.org/10.1021/es00058a006.
Hinrichs, R., Soares, M.R.F., Lamb, R.G., Soares, M.R.F., Vasconcellos, M.A.Z., 2011. Phase characterization of debris generated in brake pad coefficient of friction tests. Wear 270, 515–519. http://dx.doi.org/10.1016/j.wear.2011.01.004.
Iijima, A., Sato, K., Yano, K., Kato, M., Kozawa, K., Furuta, N., 2008. Emission factor for antimony in brake abrasion dust as one of the major atmospheric antimony sources. Environ. Sci. Technol. 42, 2937–2942. http://dx.doi.org/10.1021/es702137g.
Iijima, A., Sato, K., Yano, K., Kato, M., Tago, H., Kato, M., Kimura, H., Furuta, N., 2007. Particle size and composition distribution analysis of automotive brake abrasion dusts for the evaluation of antimony sources of airborne particulate matter. Atmos. Environ. 41, 4908–4919. http://dx.doi.org/10.1016/j.atmosenv.2007.02.005.
Inoue, M., Hara, Y., Sasada, T., 1990a. Degradation of cured phenolic resin for brake lining caused by shearing force: 1st report, molecular weight distribution of extracts. Trans. Jpn. Soc. Mech. Eng. C 56, 222–227. http://dx.doi.org/10.1299/kikaic.56.222 (in Japanese with English Abstract, Figures, and Tables).
Inoue, M., Hara, Y., Sasada, T., 1990b. Degradation of cured phenolic resin for brake linings caused by shearing force: 2nd report, Influence of metal powders. Trans. Jpn. Soc. Mech. Eng. C 56, 1614–1619. http://dx.doi.org/10.1299/kikaic.56.1614 (in Japanese with English Abstract, Figures, and Tables).
Johansson, C., Norman, M., Burman, L., 2009. Road traffic emission factors for heavy metals. Atmos. Environ. 43, 4681–4688. http://dx.doi.org/10.1016/j.atmosenv.2008.10.024.
Kukutschová, J., Moravec, P., Tomášek, V., Matějka, V., Smolík, J., Schwarz, J., Seidlerová, J., Šafářová, K., Filip, P., 2011. On airborne nano/micro-sized wear-particles released from low-metallic automotive brakes. Environ. Pollut. 159, 998–1006. http://dx.doi.org/10.1016/j.envpol.2010.11.036.
Lawrence, S., Sokhi, R., Ravindra, K., Mao, H., Prain, H.D., Bull, I.D., 2013. Source apportionment of traffic emissions of particulate matter using tunnel measurements. Atmos. Environ. 77, 548–557. http://dx.doi.org/10.1016/j.atmosenv.2013.03.040.
Lee, P., Lee, L., Filip, P., 2012. Development of Cu-free Brake Materials. SAE Int. http://dx.doi.org/10.4271/2012-01-1787.
Lough, G.C., Schauer, J.J., Park, J.-S., Shafer, M.M., Deminter, J.T., Weinstein, J.P., 2005. Emission of metal associated with motor vehicle roadways. Environ. Sci. Technol. 39, 826–836. http://dx.doi.org/10.1021/es048715f.
Mihara, T., Mochida, M., 2011. Characterization of solvent-extractable organics in urban aerosols based on mass spectrum analysis and hygroscopic growth measurement. Environ. Sci. Technol. 45, 9168–9174. http://dx.doi.org/10.1021/es201271w.
Minoura, H., Morikawa, T., Mizohata, A., Sakamoto, K., 2012. Carbonaceous aerosol and its characteristics observed in Tokyo and south Kanto region. Atmos. Environ. 61, 605–613. http://dx.doi.org/10.1016/j.atmosenv.2012.07.058.
Mohr, C., Huffman, J.A., Cubison, M.J., Aiken, A.C., Docherty, K.S., Kimmel, J.R., Ulbrich, I.M., Hannigan, M., Jimenez, J.L., 2009. Characterization of primary organic aerosol emissions from meat cooking, trash burning, and motor vehicles with high-resolution aerosol mass spectrometry and comparison with ambient and chamber observations. Environ. Sci. Technol. 43, 2443–2449. http://dx.doi.org/10.1021/es8011518.
Okayama, K., Kishimoto, H., Hiratsuka, K., 2013. Tribo-reduction of metal oxides by tribo-degradation of phenolic resin in brake pads. Trans. Jpn. Soc. Mech. Eng. C 79, 2558–2570. http://dx.doi.org/10.1299/kikaic.79.2558 (in Japanese with English Abstract, Figures, and Tables).
Oleksii, N., Mattia, A., Ulf, O., 2015. Temperature effect on emission of airborne wear particles from car brakes. Euro Brake 2015. EB2015-TEF-014.
Österle, W., Griepentrog, M., Gross, T., Urban, I., 2001. Chemical and microstructural changes induced by friction and wear of brakes. Wear 251, 1469–1476. http://dx.doi.org/10.1016/S0043-1648(01)00785-2.
Plachá, D., Peikertova, P., Kukutschova, J., Lee, P., Čabanová, K., Karas, J., Kuchařová, J., Filip, P., 2016. Identification of organic compounds released from low-metallic automotive model brake pad and its non-airborne wear particles. SAE Int. J. Mater. Manf. 9 (1) http://dx.doi.org/10.4271/2015-01-2662.
Pierson, W.R., Brachaczek, W.W., 1983. Particulate matter associated with vehicles on the road. Ii. Aerosol. Sci. Technol. 4, 1–40. http://dx.doi.org/10.1080/02786828308958610.
Quiroz, W., De Gregori, I., Basilio, P., Bravo, M., Pinto, M., Lobos, G.M., 2009. Heavy weight vehicle traffic and its relationship with antimony content in human blood. J. Environ. Monit. 11, 1051–1055. http://dx.doi.org/10.1039/b815838j.
Rakopoulos, C.D., Giakoumis, E.G., 2009. Diesel Engine Transient Operation: Appendix A. Exhaust Emission Regulations and Transient Cycles, ISBN 978-1-84882-375-4, pp. 362–368.
Sanders, P.G., Xu, N., Dalka, T.M., Maricq, M.M., 2003. Airborne brake wear debris: size distributions, composition, and a comparison of dynamometer and vehicle tests. Environ. Sci. Technol. 37, 4060–4069. http://dx.doi.org/10.1021/es034145s.
Sekimoto, K., Inomata, S., Tanimoto, H., Fushimi, A., Fujitani, Y., Sato, K., Yamada, H., 2013. Characterization of nitromethane emission from automotive exhaust. Atmos. Environ. 81, 523–531. http://dx.doi.org/10.1016/j.atmosenv.2013.09.031.
Sternbeck, J., Sjodin, A., Andreasson, K., 2002. Metal emissions from road traffic and the influence of resuspension—results from two tunnel studies. Atmos. Environ. 36, 4735–4744. http://dx.doi.org/10.1016/S1352-2310(02)00561-7.
Thorpe, A., Harrison, R.M., 2008. Sources and properties of non-exhaust particulate matter from road traffic: a review. Sci. Total Environ. 400, 270–282. http://dx.doi.org/10.1016/j.scitotenv.2008.06.007.
van der Gon, H., Gerlofs-Nijland, M., Gehrig, R., Gustafsson, M., Janssen, N., Harrison, R., Hulskotte, J., Johansson, C., Jozwicka, M., Keuken, M., Krijgsheld, K., Ntziachristos, L., Riediker, M., Cassee, F., 2013. The policy relevance of wear emissions from road transport, now and in the future—an international workshop report and consensus statement. J. Air Waste Manage. Assoc. 63, 136–149. http://dx.doi.org/10.1080/10962247.2012.741055.
Varrica, D., Bardelli, F., Dongarrà, G., Tamburo, E., 2013. Speciation of Sb in airborne particulate matter, vehicle brake linings, and brake pad wear residues. Atmos. Environ. 64, 18–24. http://dx.doi.org/10.1016/j.atmosenv.2012.08.067.
Washington State Senate Bill SB6557, 2010. An Act Relating to Limiting the Use of Certain Substances in Brake Friction Materials.
Zhang, S., Chen, W., Li, Y., 2009. Wear of Friction Material during Vehicle Braking. SAE Int. http://dx.doi.org/10.4271/2009-01-1032.
Zhao, J., Lewinski, N., Riediker, M., 2015. Physico-chemical characterization and oxidative reactivity evaluation of aged brake wear particles. Aerosol. Sci. Technol. 49, 65–74. http://dx.doi.org/10.1080/02786826.2014.998363.